The Microwave plasma process – a versatile process to synthesise nanoparticulate materials

Dieter Vollath[1,*] and D. Vinga Szabó[2]
[1]*NanoConsulting, Primelweg 3, D-76297, Stutensee, Germany;* [2]*Forschungszentrum Karlsruhe, Institut für Materialforschung III, D-76021, Karlsruhe, P.O. Box 3640, Germany; *Author for correspondence (Tel.: +49-7249678; E-mail: dieter.vollath@nanoconsulting.de)*

Key words: nanoparticles, microwave plasma, luminescence, superparamagnetism, nanocomposite, gas phase process, aerosols, coating

Abstract

The microwave plasma process inherently produces nanoparticulate powders with very narrow particle size distribution. During synthesis, the particles carry electric charges of equal sign. Therefore, by electrostatic repulsion, particle growth is reduced and agglomeration thwarted. This is shown by gas kinetic considerations and experimental results. Furthermore, this process allows coating of the particles with organic or inorganic phases, reducing interaction of different particles. This makes it possible to technically exploit properties, characteristic for isolated particles. Additionally, the coating process allows the combination of different properties such as superparamagnetism and luminescence, as it is demonstrated in different examples.

Introduction

Generally, applications of nanomaterials may be divided into two groups. The first one, with improved properties as compared to coarse-grained materials, replaces conventional materials. In most of these cases, the amount of material needed is relatively large. These applications are in fierce competition to conventional ones and potential profits are therefore limited. The other group is based on entirely new properties, to be realized only with the use of nanomaterials. In most cases, the amount of materials necessary is relatively small, and possible profits are high, as those applications usually are not price-sensitive. These considerations are summarized in Figure 1.

The requirements on materials for the second group are high. In most cases, these materials exhibit special size dependent properties. Typical examples are the blocking temperature of superparamagnetic particles depending on D^3 (D... particle diameter) or the blue shift of the luminescence of quantum dots depending on D^{-2}. These examples demonstrate that a very narrow particle size distribution is necessary. Most of the conventional routes for synthesis lead to relatively broad particle size distributions, whereas the microwave plasma process inherently leads to narrow size distributions in the product. The reason for this will be explained in this paper in comparison to conventional processes. Looking at functional nanomaterials, one has to realize that the very special properties are often ones of a single isolated particle. In many cases, it is therefore necessary to keep the particles on a certain distance to reduce interaction. This leads to the

		Price		Quantity		Profits
		low	high	small	large	
Properties	improved	X			X	questionable
	new		X	X		potentially high

Figure 1. Considerations on properties, price, quantities, and possible profits of nanoparticulate materials.

necessity of nanocomposites. The best possibility to fulfil these conditions are coated nanoparticles. It will be shown that in contrast to conventional processes, the microwave plasma process is well suited to coat nanoparticles *in situ* with a second ceramic or organic phase. The second phase used for coating may be just a distance holder or contribute an additional property. This allows combining different properties in one particle.

Synthesis

Synthesis of the ceramic particles is performed in a reaction tube passing a resonant microwave cavity. At the intersection of the reaction tube with the cavity, a plasma is ignited (Vollath & Sickafus, 1992; Vollath, 1994). Within the plasma, chemical reactions leading to the intended compounds are performed. As the reactants are dissociated and ionized in the plasma, there are no activation barriers to be overcome thermally. Therefore, the reaction temperature may be kept low. In contrast to conventional processes using gas phase reactions, where temperatures in the range from 1200 to 1500 K are applied, overall temperatures in the range from 400 to 750 K are sufficient with the microwave plasma process. Additionally, particles leaving the reaction zone carry electric charges of equal sign. Therefore, they repel each other.

To demonstrate the difference between conventional gas phase synthesis and synthesis using microwave plasma, the kinetics or particle formation must be studied. The probability for the collision of two particles or atoms with the diameter D_1 and D_2 has to be estimated.

Within a time interval Δt, a particle with the mass m passes a volume $V = D^2\bar{c}\Delta t\pi/4$.

The mean value of the velocity $\bar{c}$ of a particle depends on the particle mass m and therefore, on the particle volume, which is proportional D^3.

$$\bar{c} = \left(\frac{2kT}{m}\right)^{0.5} \propto m^{\ 0.5} \propto D^{\ 1.5} \tag{1}$$

The probability p to find, a certain particle on a well-defined point of the volume V_{total} within a time interval Δt is

$$p = \frac{V}{V_{\text{total}}} = \frac{\pi}{4}\frac{D^2\bar{c}\Delta t}{V_{\text{total}}} = K_1 D^{0.5} \tag{2}$$

with K_i representing constants, here and in the text to follow. A second particle with a different diameter will be found at the same place during the time interval Δt with the probability

$$p_{1\ 2} = p_1 p_2 = K_1^2 (D_1 D_2)^{0.5} \tag{3}$$

To obtain the collision probability, it is necessary to multiply $p_{1\ 2}$ with the concentration of the particles with diameter D_1 and D_2. In a simplified manner, the term $(D_1D_2)^{0.5}$ will be called 'collision cross-section.' Figure 2a depicts this collision cross-section as function of particle size with collision partners of different size. As expected intuitively, the probability of collision increases with increasing size of the collision partner. As larger particles move slower than smaller ones, the former show a less pronounced increase of the collision cross-section with increasing size of the collision partner. This steeper increase for larger particles makes it impossible to obtain a product within a narrow range of particle sizes.

The situation is entirely different in the case of the microwave plasma process. In this case, the particles carry electric charges; and are accelerated in the electric field of the microwaves. The physics and technology of a microwave plasma is described in detail in the book of MacDonald (1966). The energy $\Delta U_{\text{microwave}}$, added by the microwaves to thermal energy is

$$\Delta U_{\text{microwave}} = K_2 \frac{Q}{m} \frac{z}{f^2 + z^2} = K_3 \frac{Q}{D^3} \frac{z}{f^2 + z^2} \tag{4}$$

where Q is the electric charge of the particle, f the frequency of the microwaves and z the collision frequency that is proportional to the gas pressure.

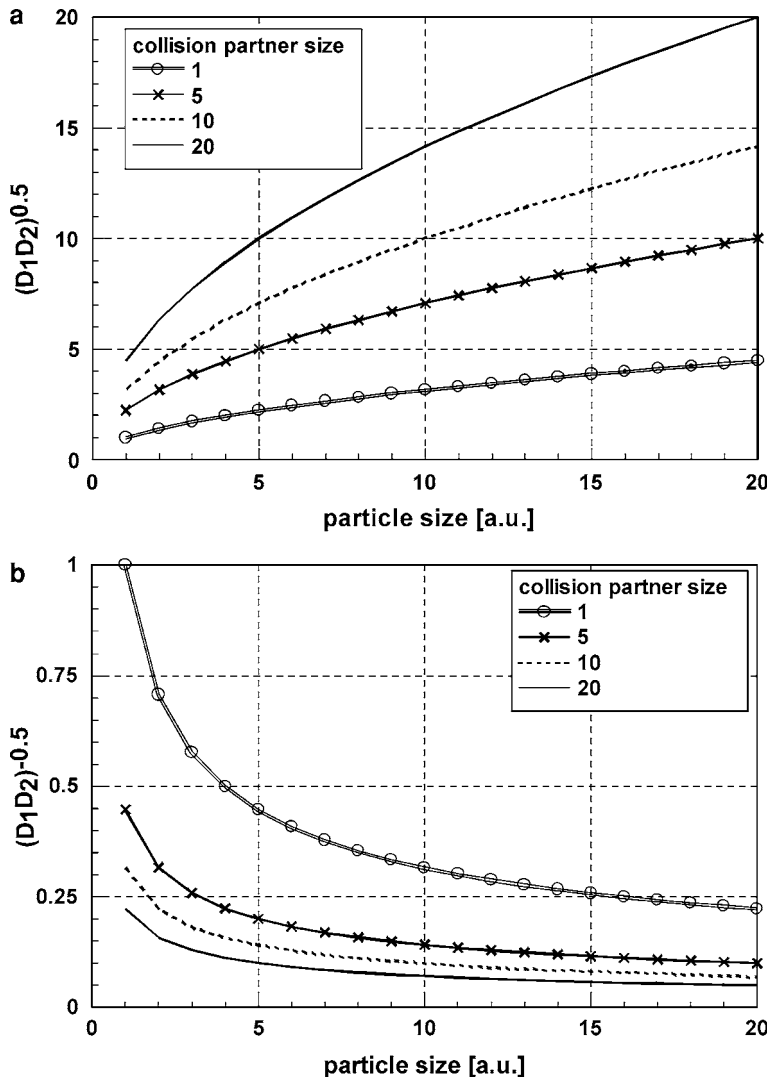

Figure 2. (a) Collision cross section for neutral particles as function of particle size with collision partners of different size. (b) Modified collision cross section for charged particles as function of particle size. In a first approximation this relationship is valid in the microwave plasma process.

The gas pressure used in the microwave plasma process is in the range from 5 to 100 mbar. This added energy leads to an increase of the temperature $\Delta T_{\text{microwave}}$ of the particles. Up to a gas pressure, where the collision frequency is equal to the microwave frequency, the energy transferred to the particles increases with increasing gas pressure. As the transferred energy is inversely proportional to the mass of the charged particles, free electrons gain significant energy. In a resonant microwave cavity, as it is applied for microwave plasma synthesis, the electric field strength is significantly above 10^4 Volt cm ^{1}. Furthermore, the electrons gain enough energy to ionise the particles. The probability for a recombination of the high energetic electrons with the ionised, positively charged particles is small. Due to the large electric field, the energy of the heavy particles is also increased significantly above the thermal mean value. The particles carry electric charges of equal sign; therefore, they repel each other. As mean value, it is assumed that the electric charging of the

particles goes up to a level of constant electric potential. This results in $Q/D = \text{const}$. Otherwise a charge transfer between the particles to equalize the electric potential will occur. This assumption is experimentally well proven. Ziemann et al. (1996) showed that the electric charge Q of aerosol particles is proportional to the particle diameter D.

The electrostatic repelling force of two charged particles in a distance r is ruled by Q_1Q_2/r^2. This force results in an acceleration Q_1Q_2/mr^2. This reduces the velocity of the particles and therefore, the collision volume passed in the time interval Δt. An exact solution of this problem leads to formulae that are, in this context, difficult to handle. However, for qualitative purposes, in a first approximation, the reduction of the collision volume can be described by the factor $1/Q_1\ Q_2$. As the charge of the particles is proportional to the diameter, the collision probability is reduced by the factor $1/D_1\ D_2$. This leads to the following modified collision cross-section:

$$p_{1\ 2} = p_1 p_2 = K^2 (D_1 D_2)^{0.5} \frac{1}{D_1 D_2} = K^2 (D_1 D_2)^{\ 0.5} \tag{5}$$

The consequences of this repulsion are visible in Figure 2b, where the modified 'collision cross-section' is plotted *versus* particle size for different collision partners. In contrast to Figure 2a, a continuous decrease of the collision cross-section with increasing size of the collision partner is also observed. Looking at particles of the size 5 and more, in the case of charged particles, the collision cross-section is more than one order of magnitude smaller as compared to neutral particles. Comparing Figure 2a and b explains why it is possible to produce nanoparticles with extremely narrow particle size distribution using the microwave plasma process. Furthermore, it demonstrates that it is nearly impossible to produce nanopowders outside of a narrow range of very small particle sizes. To obtain a comparably narrow particle size distribution using a conventional process, it is necessary to shorten the reaction time to reduce the possibility of particle growth and agglomeration.

Until now, the mass dependent transfer of energy in the E-field of the microwaves was not taken into account in the considerations above. The energy $\Delta U_{\text{microwave}}$, added to thermal energy by the microwaves leads to an increase of the temperature $\Delta T_{\text{microwave}}$ of a particle:

$$\Delta T_{\text{microwave}} = \frac{\Delta U_{\text{microwave}}}{k} = K_4 \frac{Q}{D^3} = K_5 D^{\ 2} \tag{6}$$

Considering the above, a rough approximation of the collision parameter for two particles of different size in a microwave field is given by

$$p_{1\ 2} = \frac{V_1 V_2}{V_{\text{total}}^2} = K \frac{D_1^2 D_2^2}{V_{\text{total}}^2} \left(\frac{2kT + K_6 D_1^{\ 2}}{m_1} \right)^{0.5} \times \left(\frac{2kT + K_6 D_2^{\ 2}}{m_2} \right)^{0.5} \frac{1}{D_1 D_2}, \tag{17}$$

or

$$p_{1\ 2} = K \frac{1}{V_{\text{total}}^2} \left(2kT + K_6 D_1^{\ 2}\right)^{0.5} \times \left(2kT + K_6 D_2^{\ 2}\right)^{0.5} (D_1 D_2)^{\ 0.5} \tag{18}$$

It is obvious that the influence of the energy added by the microwaves decreases with increasing mass of the particles. Therefore, it further enhances the charge-induced effect of a reduced collision probability of larger particles described above.

As mentioned in the introduction, conventional processes apply quite high temperatures. At these temperatures, some ionisation of the particles by thermal electron emission will occur. One has to check the influence of this phenomenon on the process of particle formation. Assuming a concentration c_{charged} of charged particles, there is a probability of c^2_{charged} for an encounter of two charged particles. The collision cross-section in such a system is assumed to be a linear superposition of the ones for neutral and for charged particles. Figure 3 shows the collision cross-section for a particle with the size 5 with other particles using Eqs. (3) and (4). It is quite obvious that even a reduction from 100% ionisation to 90% ionisation leads to an increase of the collision cross-section. This allows the conclusion that partial ionisation of the particles improves the size distribution of the product. However, full advantage is obtained only if almost all the particles carry electric charges.

The influence of particle charge can be demonstrated by quenching it during synthesis. This is done by adding water to the reaction gas. In this case, $(OH)^-$ ions stemming from dissociated water neutralize the particles by the following process:

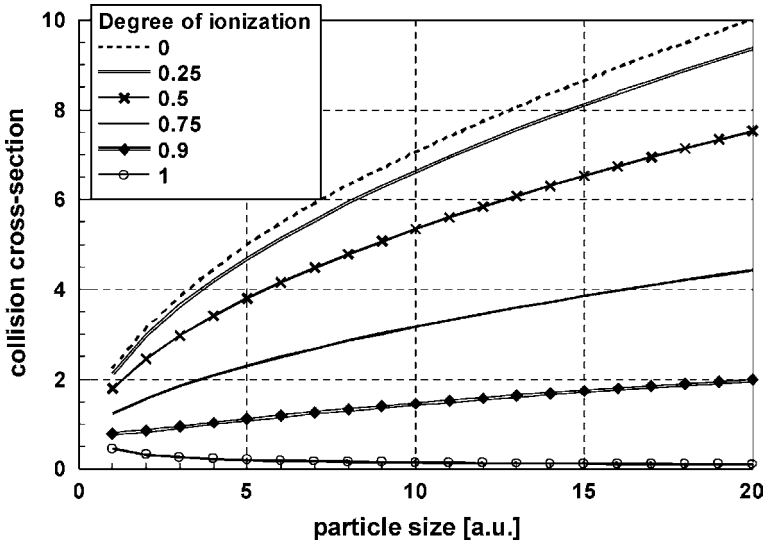

Figure 3. Collision cross section for a particle of size 5 with other particles as function of particle size, considering different degrees of partial ionization of the particles.

$$H_2O \Rightarrow H^+ + (OH)$$

$$\text{particle}^{n+} + n(OH) \Rightarrow (\text{particle}^{n+} + n(OH))^{\text{neutral}}$$

Now, the neutralized particles carry a hydroxide layer at the surface. Figures 4a and b demonstrate the drastic influence of water additions to the reaction gas on the synthesis product. Figure 4a shows ZrO_2 synthesized without additions of water, whereas the material depicted in Figure 4b was produced under similar conditions, except for water additions to the reaction gas. In this example, zirconia produced without additions of water show a grain size around 8 nm. Most of the grains are of equal size. In contrast, the material produced with water additions is characterized by a broad distribution of particle sizes in the range from 10 to 50 nm. This dramatic difference between these two batches of material is caused by the neutralization of the nanoparticles due to the water added to the reaction gas. On the other hand, if the reactants obtain a high degree of ionisation in the plasma, nucleation and growth of particles may be difficult or even inhibited. In special cases, this may lead to a reduced probability of nucleation with the consequence of either extremely small particles or reduced efficiency in the production process. In the latter case, one has to search for better-suited precursors. A typical example for extremely small particle sizes is given in Figure 5. This figure shows the particle size spectrum of zirconia determined by particle mass spectrometry (Roth, 2000). The graph clearly demonstrates a narrow particle size distribution. A distribution like that cannot be obtained by thermal gas phase reactions.

After synthesis, the particles leave the reaction zone carrying electric charges. Therefore, the probability for agglomeration is significantly reduced. This makes it possible to coat these particles in a second reaction step. This coating may consist either of a second ceramic phase or an organic one (Vollath & Szabó, 1994; Vollath et al., 1998). Typical examples of coated composites are shown in Figures 6 and 7. The particles in Figure 6 consist of hafnia and are coated with alumina. The lattice fringes indicate crystallized hafnia cores, whereas the alumina coating is amorphous. If the particles would not repel each other in such a coating process this would lead to coated agglomerates, unless the particle concentration in the gas phase is small enough to exclude collisions of two or more particles. As the temperatures during synthesis are relatively low, the particles leave the reaction zone in a temperature regime allowing coating with organic phases. In the simplest case, an organic coating consists of a polymer used as distance holder (Vollath & Szabó, 2002). This polymer is selected according to the properties needed for application. In most cases,

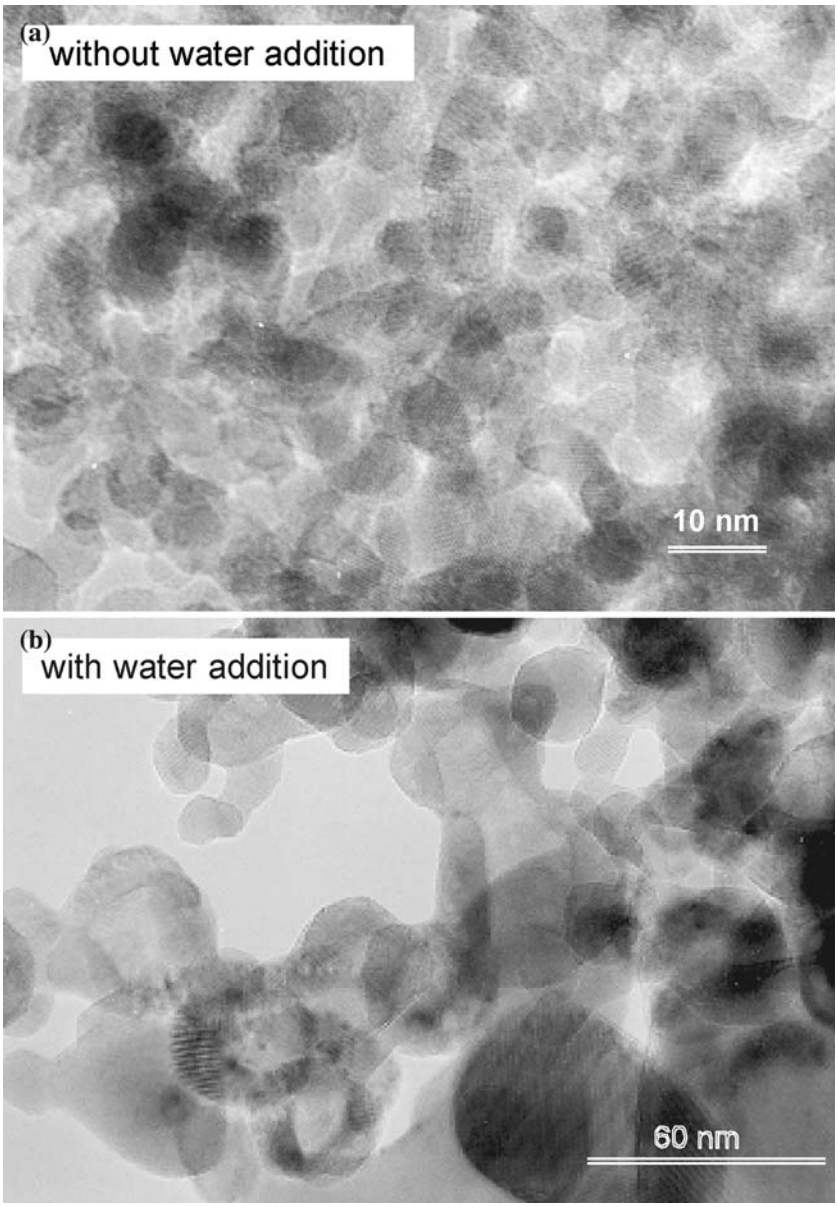

Figure 4. (a) Transmission electron micrograph of nanosized ZrO_2 synthesized in a microwave plasma without water addition. The particle size is around 8 nm. (b) Transmission electron micrograph of nanosized ZrO_2 synthesized in a microwave plasma with water addition. The particle size is in the range from 10 to 50 nm.

PMMA, made of MMA (methylmethacrylate, $H_2C=C(CH_3)CO–O–CH_3$) as monomer, is appropriate. A highly hydrophilic surface is obtained using HPMA (poly hydroxypropylmethacrylate, made of $H_2C=C(CH_3)CO–O–(C_3H_6)–OH$)). In both cases, the particles pass the vapour of the monomer that condenses at the surface of the particle. Under the influence of the UV-radiation of the plasma, the monomer molecules at the surface polymerise. Highly hydrophobic surfaces are obtained by using evaporated $C_{20}F_{42}$ for coating. As shown below, even more extreme functionalisation of the particle surface with organic material is possible. Additionally, by

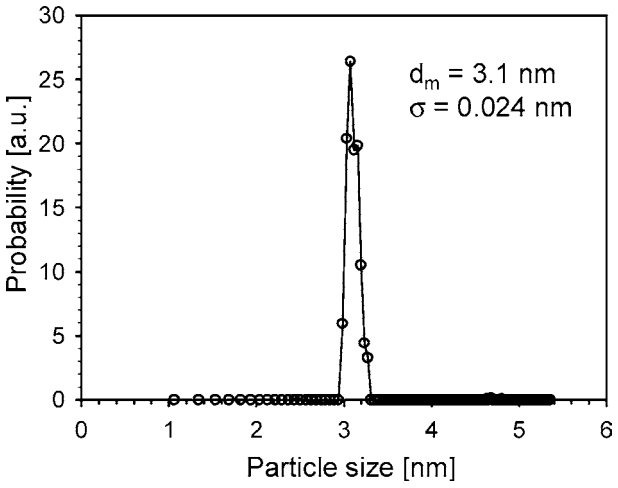

Figure 5. Particle size distribution for ZrO_2 nanoparticles measured *in situ* by particle mass spectrometry (Roth, 2000).

proper selection of the reactants, the interface between ceramic kernel and organic layer may contribute special properties.

A typical example for polymer coated ceramic particles is shown in Figure 7. In this figure, depicting Fe_2O_3 particles coated with PMMA, one observes ceramic particles with sizes in the range from 5 to 6.5 nm, each one coated separately with a ca. 3 nm thick PMMA layer. It can be seen clearly that the ceramic cores of the particles never touch each other. However, it is unavoidable that the coated particles are in contact, as during the

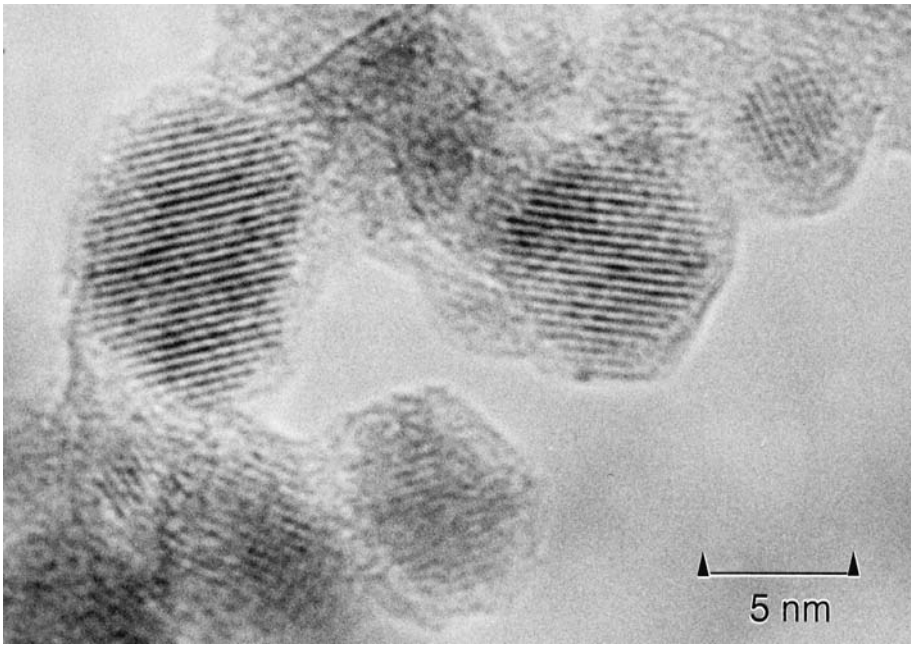

Figure 6. High resolution transmission electron micrograph of HfO_2/Al_2O_3 nanoparticles. The hafnia core, characterized by lattice fringes, is crystallized; the alumina coating is amorphous.

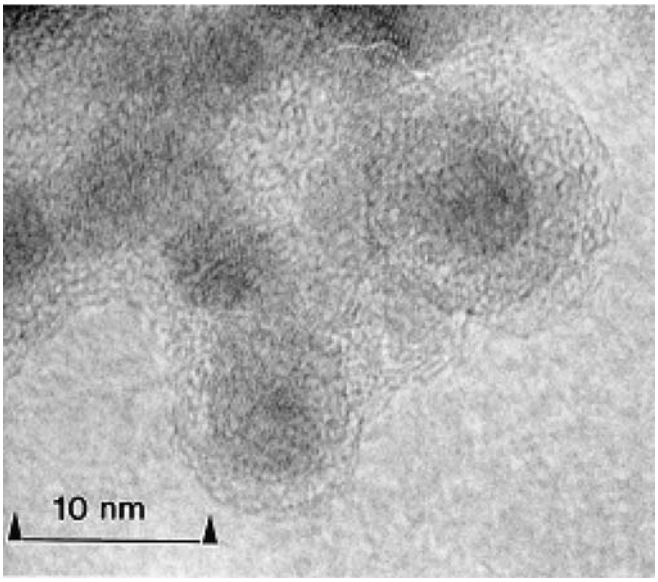

Figure 7. Transmission electron micrograph of ceramic/polymer nanoparticles. The core is crystalline, superparamagnetic γ Fe_2O_3 with sizes around 5 6.5 nm, the coating consists of PMMA with a thickness of approximately 3 nm.

coating process with an organic phase further ionization of the particles does not occur.

Properties of some special nanocomposites

Luminescence

Coating of nanoparticles allows synthesis of nanocomposites with very special properties. Typical examples for these properties are luminescence and magnetism. Usually, luminescence of nanoparticles is attributed to quantum confinement phenomena. Most materials used for quantum dots are quite problematic with respect to application. The best ones, particles based on selenides or sulphides of cadmium and zinc are highly toxic and to some extent cancerous. Others, like ZnO, are unstable and loose their luminescence properties due to the formation of hydroxides at the surface. Nanocomposites, in particular ceramic/polymer nanocomposites, overcome some of these problems. In the case of zinc oxide, coating the surface with PMMA or PTFE prevents the uptake of water at the surface (Vollath et al., 2002). Additionally, coating of the surface with a polymer may create new properties.

Particles of wide gap insulators, such as ZrO_2, HfO_2, Al_2O_3, etc. coated with PMMA show luminescence if excited with UV-light. This is astonishing, as the band gap of these materials is around 8 eV, whereas UV-energy of 3.5 eV is sufficient for excitation of this luminescence. As it is shown in Figure 8, the emission spectra of these composites are independent of the oxide core. Besides the emission line around 420 nm, this graph shows the exciting line at 325 nm in first order and at 650 nm in second order. The emission of these composites shows blue shift, like the emission of quantum dots. In quantum dots blue shift follows a dependency as $\Delta/(1/\lambda) \propto D^{\alpha}$. For quantum confinement, theoretically the value of the exponent α should be 2 (Brus, 1984) or 3 (Monticone et al., 1998). Experimentally, α was found to vary between 1 and 6 (Micic et al., 1996; Fu & Zunger, 1997; Albe et al., 1998; Sun et al., 2001). In the oxide/PMMA systems, these relations are fundamentally different. In this system, the relation $\Delta/(1/\lambda) \propto D^3$ was found for blue shift, indicating an entirely different mechanism. The polymer coating is chemically bonded to the oxide core, as it is outlined in Figure 9. The crucial point is that the polymer molecules at the surface undergo partial loss of ester groups under formation of carboxylate bonds to the particle surface

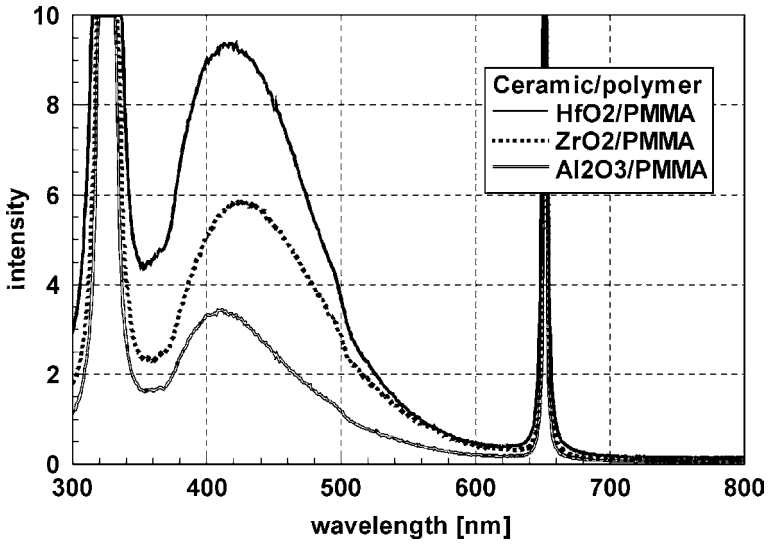

Figure 8. Luminescence spectra of ceramic/polymer nanopowder excited with UV light. The cores consist of the wide gap insulators HfO_2, ZrO_2, or Al_2O_3, respectively. In all cases, the coating is made of PMMA.

(Lamparth et al., 2002). It was shown that the carbonyl group directly adjacent to the oxide surface is responsible for the light emission (Vollath et al., 2004).

The idea of coated particles is expandable to broader applications. It is possible to coat the surface of the ceramic particle with an organic lumophore. This leads to a particle design as it is depicted in Figure 10. This design opens the possibility of applying a vast amount of organic lumophores in nanotechnology. Additionally, different properties can be combined in one nanoparticle. For example, it is possible to use magnetic material for the ceramic core, to add a luminescent layer, and to coat with a polymer a second time. This polymer may be hydrophilic, hydrophobic, or may have any other functionalization needed in biotechnology or any other application. Placing a

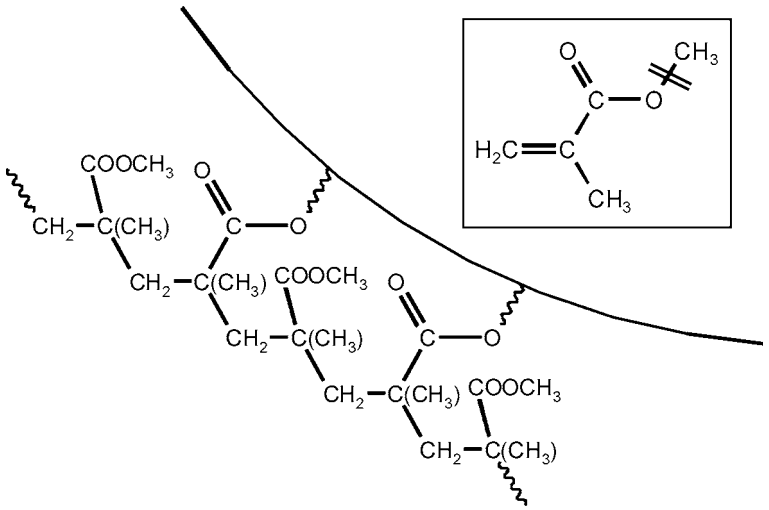

Figure 9. Model of the bonding of PMMA at the surface of oxide nanoparticles. The insert shows the structure of an MMA molecule. The bond at which the CH_3 group is cleaved is indicated.

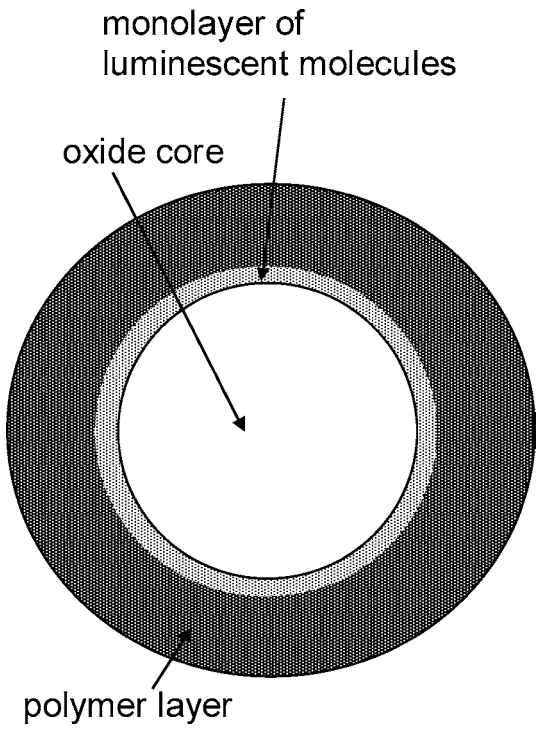

Figure 10. Model of a luminescent nanoparticles consisting of a ceramic core, a monolayer of organic lumophore and an outer polymer layer for protection.

monolayer of an organic lumophore at the surface of nanoparticles adds the possibility of additional features stemming from the interaction between these phases. This can clearly be seen on the example of a nanocomposites particle consisting of a zirconia core, anthracene as lumophore and PMMA as surface coating. Figure 11 exhibits spectra of pure anthracene and the before mentioned composite. Obviously, the spectra are different. The composite shows the spectrum of anthracene and additionally a very strong line at 422 nm. This line is observed independently of the composition of the ceramic core but never found in the pure organic phase.

Magnetism

It is well known that magnetic properties are grain size dependent. Large grains in the range of micrometers are subdivided into magnetic domains by Bloch-walls. Reducing the grain size leads to dimensions, where each grain consist of only one domain. These single domain particles exhibit high coercitivity and remanence. Technically, these materials are used for magnetic information storage. Further reduction of the grain size leads to a point, where coercitivity and remanence vanish (Jacobs & Bean, 1963). Now the material is superparamagnetic. Superparamagnetism is characterized by an energy of anisotropy KV (K is the constant of anisotropy of the material, V, the volume of the particle)

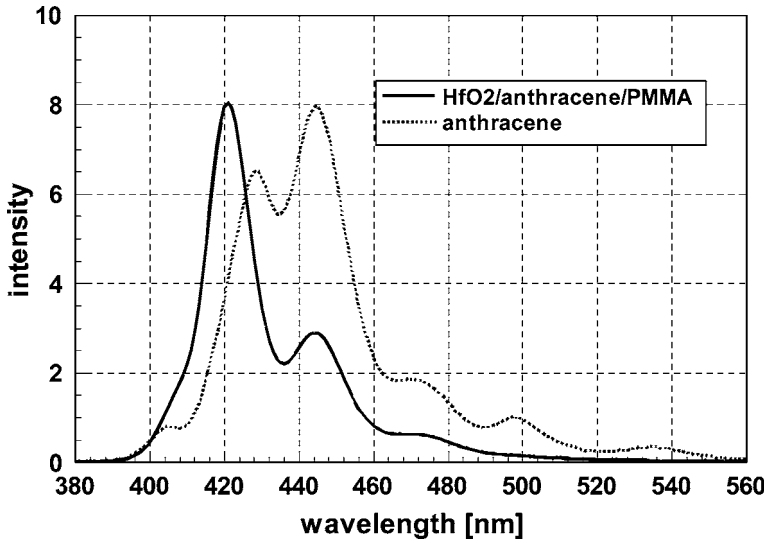

Figure 11. Luminescence spectra of pure anthracene and lumophore nanoparticles consisting of a HfO_2 core, a monolayer of anthracene and a PMMA coating. Please note the strong additional emission at 420 nm.

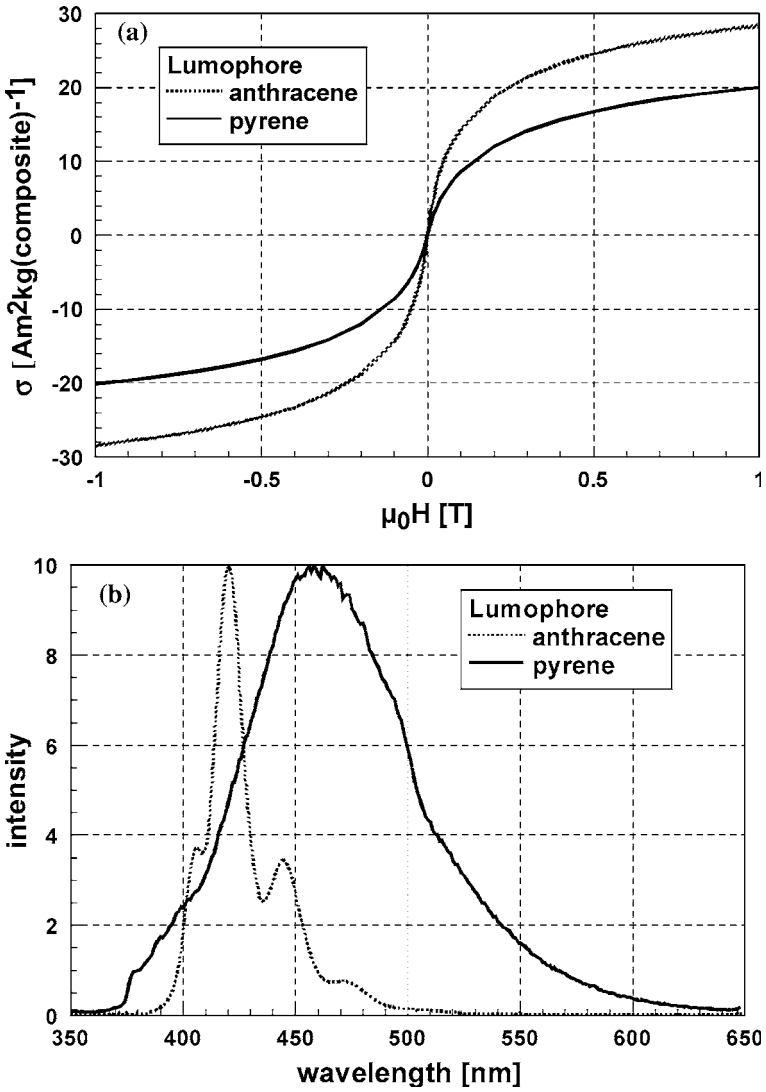

Figure 12. (a) Magnetization curves of two superparamagnetic luminescent nanocomposites. The first nanocomposite consists of a γ Fe_2O_3 core, anthracene and PMMA; the second one contains pyrene as lumophore. (b) Luminescence spectra of different γ Fe_2O_3/lumophore/PMMA nanoparticles.

keeping the vector of magnetization in a certain direction which is smaller than thermal energy kT. Therefore, the condition $KV < kT$ must be fulfilled (Néel, 1949). The temperature $T_B = KV/k$, at which both energies are equal is called 'blocking temperature.' Above blocking temperature, coercitivity and remanence are nil. These considerations are valid for one single particle or an arrangement of particles, where the particles are kept on sufficient distance to reduce interaction. Interacting superparamagnetic particles loose this special property.

In Figure 12, magnetization curves of two superparamagnetic nanocomposites are shown. To demonstrate a combination of properties, these composites contain an additional layer of a lumophore. Anthracene and pyrene were selected as lumophores, respectively. The difference in magnetization visible in Figure 12a is caused by the different sizes of the magnetic nanoparticles

and is not influenced by the lumophore. Magnetic particles have a surface layer with a thickness of approximately 1 nm that does not contribute to magnetization. This reduces magnetization essentially. For example, specimens consisting of 5 nm particles have at most ca. 50% of the saturation magnetization as compared to coarse-grained material. Figure 12b displays the luminescence spectra of the specimen used for Figure 12a. This is an example for a nanocomposite material exhibiting two physical properties in one composite particle, which would never be found together in one material.

Conclusion

The microwave plasma process inherently produces particles with very narrow size distribution. This phenomenon has been attributed to unipolar particle charge during synthesis and qualitatively explained using simplified gas kinetic considerations. Due to these charges, the particles repel each other, limiting particle growth and thwarting agglomeration. As the electric charge of the particles increase with increasing particle size, the probability for particle agglomeration decreases with increasing particle diameter. Experimental results confirm these considerations. This process also allows coating of the particles with a second inorganic or organic phase. The possibility of coating allows design and synthesis of particles incorporating different physical or chemical properties. This was demonstrated by the combination of magnetism and luminescence in one nanoparticle. Additionally, coating reduces the interaction between the particles. This allows e.g., to produce superparamagnetic sintered bodies.

References

Albe V., C. Jouanin & D. Bertho, 1998. Phys. Rev. B 58, 4713.

Brus L.E., 1984. J. Chem. Phys. 80, 4403.

Fu H. & A. Zunger, 1997. Phys. Rev. B 55, 1642.

Jacobs, I.S. & C.P. Bean, 1963. In: Rado G.T. & Suhl H. eds. Magnetism. Academic Press, New York, 271ff pp.

Lamparth I., D.V. Szabó & D. Vollath, 2002. Marcomol. Symp. 181, 107.

MacDonald A.D., 1966. Microwave Breakdown in Gases. New York: John Wiley & Sons.

Micic O.I., J. Sprague, Z. Lu & J. Nozik, 1996. Appl. Phys. Lett. 73, 3150.

Monticone S., R. Tufeu & A.V. Kanaev, 1998. J. Phys. Chem. B 102, 2854 2862.

Néel L., 1949. Comt. Rend. 228, 664.

Roth P. 2000, private communication.

Sun C.Q., T.P. Chen, B.K. Tay, S. Li, H. Huang, Y.B. Zhang, L.K. Pan, S.P. Lau & X.W. Sun, 2001. J. Phys. D 34, 3470 3479.

Vollath D. & K.E. Sickafus, 1992. NanoStruct. Mater. 1, 427.

Vollath D., 1994. Mat. Res. Soc. Symp. Proc. 347, 629.

Vollath D. & D.V. Szabó, 1994. NanoStruct. Mater. 4, 927.

Vollath, D., D.V. Szabó & B. Seith, 1998. German Patent DE19638601C1.

Vollath, D. & D.V. Szabó, 2002. In: K.L. Choy, ed. Innovative Processing of Films and Nanocrystalline Powders. Imperial College Press, London.

Vollath D., I. Lamparth & D.V. Szabó, 2002. Mat. Res. Soc. Symp. Proc. 703, V7.8.1.

Vollath D., D.V. Szabó & S. Schlabach, 2004. J. Nanoparticle Res. 6, 181.

Ziemann P.J., D.B. Kittelson & P.H. McMurry, 1996. J. Aerosol Sci. 27(4), 587.